

# Variation in the Optical Sensing Responses toward Vapors of a Porphyrin/Phthalocyanine Hybrid Thin Film

J. Spadavecchia and G. Ciccarella

*Dip. Ingegneria dell'Innovazione, Università di Lecce, campus universitario,  
Via per Arnesano, 73100 Lecce, Italy*

T. Stomeo

*ISUFI–Istituto Superiore Universitario per la Formazione Interdisciplinare,  
Università di Lecce, campus universitario, Via per Arnesano, 73100 Lecce, Italy*

R. Rella,\* S. Capone, and P. Siciliano

*Istituto per la Microelettronica e i Microsistemi IMM-CNR, Sezione di Lecce,  
campus universitario, via Arnesano, 73100 Lecce, Italy*

*Received September 17, 2003. Revised Manuscript Received March 9, 2004*

Spin-coated layers of zinc(II) tetra-4-(2,4-di-*tert*-amylphenoxy)phthalocyanine (ZnPc<sup>tamyl</sup>) and copper(II) tetrakis(*p-tert*-butylphenyl)porphyrin (CuP<sup>tphen</sup>) have been synthesized and used as solid state chemically interacting materials deposited in thin film form for the detection of alcohols, amines, ketones, alkanes, and pyridines for applications in food quality control. The UV–Vis variations obtained by the exposure of the sensing layers to the mentioned analytes in controlled atmosphere have been analyzed and compared with those deriving by a single thin film obtained by mixing the two metal complexes in an appropriate ratio. A multichannel monitoring of the main bands of the sensing layer due to the interaction with the analyte vapors became the basis to construct a set of independent sensors located on a single sensing element. The effects in the variation of the absorption bands of the blend system are compared with the variations in absorbance observed with the two sensing layers fabricated separately with each single compound. The interaction between some volatile organic compound species and the heterogeneous sensing layer shows a different behavior in the responses with respect to the results obtained with each single compound.

## 1. Introduction

Phthalocyanines and porphyrins represent a large family of functional molecular materials with high chemical and thermal stability. These compounds are the object of great interest of chemists, physicists, and industrial scientists because of their potential role in emerging technologies, including photoconductors, solar cells, and chemical sensors.<sup>1–3</sup> These compounds, when deposited as thin films, interact with some inorganic gases such as H<sub>2</sub>S, HCl, Cl<sub>2</sub>, NH<sub>3</sub>, or NO<sub>x</sub> by absorption onto the sensing layer.<sup>4–6</sup> This phenomenon leads to

changes of some physical properties of the thin films that can be monitored by different transduction methodologies such as quartz microbalances, surface acoustic wave sensors, surface plasmon resonance, and conductivity measurements of the chemical sensing layers.<sup>7,8</sup>

To this purpose metallophthalocyanines and metalloporphyrins became a natural choice for the optical detection of volatile organic compounds because of their large spectral shifts upon ligand binding and their intense coloration. Using metal centers that span a range of chemical “hardness” and ligand-binding affinity, a wide range of volatile analytes might be detectable. Moreover, porphyrins show significant solvatochromic effects, even when they interact with vapors (for example, alcohols, amines, phosphines, arenes, ketones), showing distinguishable colorimetric effects.<sup>9,10</sup> Furthermore, the response toward specific VOCs (volatile organic compounds) can be finely tuned by simple

\* Corresponding author. E-mail: roberto.rella@imm.cnr.it.

(1) Leznoff, C. C.; Lever, A. B. P. *Phthalocyanine Properties and Applications*; VCH: Weinheim, 1989; pp 1–3.

(2) Whitlock, J. B.; Panayotatos, P.; Sharma, G. D.; Cox, M. D.; Sauers, R. R.; Bird, G. R. *Opt. Eng.* **1993**, *32*, 1921–1934; Rella, R.; Siciliano, P.; Valli, L.; Spaeth, K.; Gauglitz, G. *Sens. Actuators, B* **1998**, *48*, 328; Rodriguez-Mendez, M. L.; Gorbunova, Y.; De Saja, J. A. *Langmuir* **2002**, *18* (24), 9560–9565; Gorbunova, Y.; Rodriguez-Mendez, M. L.; Kalashnikova, I. P.; Tamilova, L. G.; De Saja, J. A. *Langmuir* **2001**, *17* (16), 5004.

(3) Crooks, R. M.; Ricco, A. J. *Acc. Chem. Res.* **1998**, *31*, 219–227.

(4) Capone, S.; Rella, R.; Siciliano, P.; Valli, L. *Langmuir* **1998**, *15*, 1748–1752.

(5) Dooling, C. M.; Worsfold, O.; Richardson, T. H.; Tregonning, R.; Vysotsky, M. O.; Hunter, C. A.; Kato, K.; Shinbo, K.; Kaneko, F. *J. Mater. Chem.* **2001**, *11*, 392.

(6) Richardson, T.; Smith, V. C.; Johnstone, R. A. W.; Sobral, A. J. F.; D'A Rocha-Gonsalves, A. M. *Thin Solid Films* **1998**, *327–329*, 315.

(7) Burl, M. C.; Doleman, B. J.; Schffer, A.; Lewis, N. S. *Sens. Actuators, B* **2001**, *72*, 149.

(8) Paolesse, R.; Di Natale, C.; Dall'Orto, V. C.; Magagnano, A.; Angelaccio, A.; Motha, N.; Sgarlata, A.; Resano, I.; Marcini, M.; D'Amico, A. *Thin Solid Films* **1999**, *354*, 245–250.

(9) Rakow, N. A.; Suslick, K. S. *Lett. Nature* **2000**, *406*, 710–713.

(10) D'Amico, A.; Di Natale, C.; Paolesse, R.; Magagnano, A.; Mantini, A. *Sens. Actuators, B* **2000**, *B65*, 209–215.

modification on the molecule skeleton through the substitution of atoms or ligands.<sup>11</sup> The optical detection of gases and vapors can represent an appealing alternative and the adoption of organic spin-coated films as sensing layer permits the exploration of the sensitivity and selectivity dependence on the molecular structure through structural modulation. The large panorama of the organic dyes offers various possibilities, but there are some advantages in using phthalocyanines and porphyrins as sensing compounds, due to their spectral features.<sup>12,13</sup>

It is important to underline that UV–Vis spectra of phthalocyanines are typically described by two main absorption bands located in the UV–Vis spectral range: the Q bands centered respectively at about 680 and 620 nm and the B band centered at about 350 nm. Whereas, porphyrins have an intense absorption band centered in the 400–420 nm spectral region.<sup>14</sup>

Thin films of these compounds are generally prepared by chemical or physical methods based on such techniques as vapor deposition, spin coating, and Langmuir–Blodgett (LB) deposition.<sup>15,16</sup> In our case, the spin coating method has been adopted in order to realize a reproducible, open structure with a high surface/volume ratio. So, a high presence of absorption sites disposable for the vapor/active layer interaction can be obtained.

In a previous work<sup>17</sup> we reported on the spin-coated thin films of two differently substituted metallophthalocyanines suitable to construct reversible optical sensor devices in the UV–Vis spectral range. Monitoring of the variations in their absorption spectra induced by the exposure to the headspace of different VOCs allowed us to observe the linearity of the response at various concentrations. In continuation of our work and to enhance the selectivity toward various classes of volatile organic compounds (alcohols, amines, ketones, alkanes, pyridines), we found that the fabrication of a thin sensing layer realized by using a ZnPc<sup>tamyl</sup>/CuP<sup>tphen</sup> mixture played a determinant role in the realization of a multisensing system. In fact, to realize an optical sensor array using a single suitable material, we observed that the UV–Vis absorption spectrum of CuP<sup>tphen</sup> is fully integrated with that of ZnPc<sup>tamyl</sup>, because of the absence of band overlap. So, a phthalocyanine–porphyrin blend was used as a multisensing system, and the variations in the absorption spectra corresponding to the typical absorption peaks in the UV–Vis range in the presence of various VOCs of interest in food analysis were investigated. In particular, in our investigation we considered analyte compounds that are representative of different classes of chemical species. Amines are a group of biologically

active and even toxic compounds that are of great interest due to the environmental problem manifested in agriculture, where they are used in fertilizers, or in waste water, where they result from the surfactant-, pharmaceutical-, and dye-manufacturing industries. Amines play an important role in food technology; the concentration of amines is a quality criterion for food and beverages, such as banana, cheese, fish, or wine. Ketones are also present in flavor/fragrances related to many food products such as cooking oils or natural bee honey and are also involved in fats deterioration processes. But also organic acids are commonly present in foods, beverages, and medicines.

The optical responses of ZnPc<sup>tamyl</sup>, CuP<sup>tphen</sup>, and ZnPc<sup>tamyl</sup>–CuP<sup>tphen</sup> mixed thin films toward selected VOCs in specific spectral ranges have been successively analyzed by a typical unsupervised pattern recognition method like principal component analysis (PCA) in order to evaluate the discrimination power of the sensing system. PCA is a powerful unsupervised linear data analysis technique widely used in the gas-sensing area with the main aim to reduce the data space dimension. It extracts the main relationships in the data matrix containing the sensor responses and provides qualitative useful results for pattern recognition.

## 2. Experimental Section

All the chemicals tested as VOCs were purchased from Aldrich Chemical Co. and used as received without further purification; all the solvents were HPLC grade. UV–Vis solution spectra were recorded on a Varian Cary 100 scan UV–Vis spectrophotometer. Zinc(II) tetra-4-(2,4-di-*tert*-amylphenoxy)phthalocyanine (ZnPc<sup>tamyl</sup>) and copper(II) tetrakis(*p*-*tert*-butylphenyl)porphyrin (CuP<sup>tphen</sup>) were synthesized as previously reported.<sup>18–20</sup> In Figure 1 the structures of the two employed macromolecules are reported.

All the sensing layers were prepared in thin film form by spin coating on suitably cleaned quartz substrates. In particular, ZnPc<sup>tamyl</sup> spin-coated thin films were prepared by using chloroform as solvent (12 mg mL<sup>-1</sup>,  $8.0 \times 10^{-3}$  M) and by spinning the solution onto quartz substrates at 2000 rpm for 30 s. Under the same conditions, a 5 mg mL<sup>-1</sup> ( $5.6 \times 10^{-2}$  M) chloroform solution of CuP<sup>tphen</sup> gave the second coating film. The thin layers exhibited blue-green and red colors, respectively, and comparable absorption intensities. Moreover, a mixed layer (ZnPc<sup>tamyl</sup>/CuP<sup>tphen</sup>) was obtained by spinning at 2000 rpm for 30 s 2 mL of a chloroform solution containing 12 mg of ZnPc<sup>tamyl</sup> and 1 mg of CuP<sup>tphen</sup>. The thickness of all sensing layers was measured by a Tencor  $\alpha$ -step profilometer and it was about 100 nm for all investigated thin films.

The atomic force microscopy (AFM) analysis of the spin-coated films onto quartz substrates was performed by an Easy Scan E-DFM system operating in air in contact mode with a Si tip whose force constant was 0.2 N/m. Several scan sizes ranging from  $10 \mu\text{m} \times 10 \mu\text{m}$  down to  $5 \mu\text{m} \times 5 \mu\text{m}$  were recorded from different regions of the film in order to check the morphology.

Absorption spectra carried out on spin-coated films deposited onto quartz substrates were measured by using a Varian Cary 500 UV–Vis–NIR spectrophotometer. All the optical sensing tests were performed by using a filtered light source from an AVANTES tungsten–halogen lamp guided into an

(11) Di Natale, C.; Paolesse, R.; Macagnano, A.; Mantini, A.; Mari, P.; D'Amico, A. *Sens. Actuators, B* **2000**, *B68*, 319–323.

(12) Walton, D. J.; Drake, P. L.; Peterson, I. R.; Bradford, A.; Worsfold, O.; Schreeder, J.; Parry, D. A.; Forkan, M. G.; Malin, C.; MacCraith, B. D.; *Synth. Met.* **2000**, *109*, 91–96.

(13) Akrajas, M. M.; Salleh, Y.; Muhammad, *Sens. Actuators, B* **2002**, *B85*, 191.

(14) Supriyatno, H.; Yamashita, M.; Nakagawa, K.; Sadaoka, Y. *Sens. Actuators, B* **2002**, *B85*, 197–204.

(15) Rodriguez-Mendez, M. L.; Souto, J.; de Saja, R.; Martinez, J.; de Saja, J. A. *Sens. Actuators, B* **1999**, *B58*, 544–551.

(16) Zhu, D. G.; Chui, D. F.; Petty, M. C.; Harris, M. *Sens. Actuators, B* **1993**, *B12*, 111–114.

(17) Rella, R.; Spadavecchia, J.; Ciccarella, G.; Siciliano, P.; Vasapollo, G.; Valli, L. *Sens. Actuators, B* **2003**, *B89*, 86–91.

(18) Lindsey, J. S.; Schreiman, I. C.; Hsu, H. C.; Kearney, P. C.; Marguerettaz, A. M. Rothmund and Adler-Longo *J. Org. Chem.* **1987**, *52*(5), 827–836.

(19) Sakthitharan S.; Christine E.; Boyle, R. W. *Tetrahedron* **2000**, *56*, 1025–1046.

(20) Spadavecchia, J.; Ciccarella, G.; Buccolieri, A.; Vasapollo, G.; Rella, R. *J. Porphyrins Phthalocyanines*, in press.

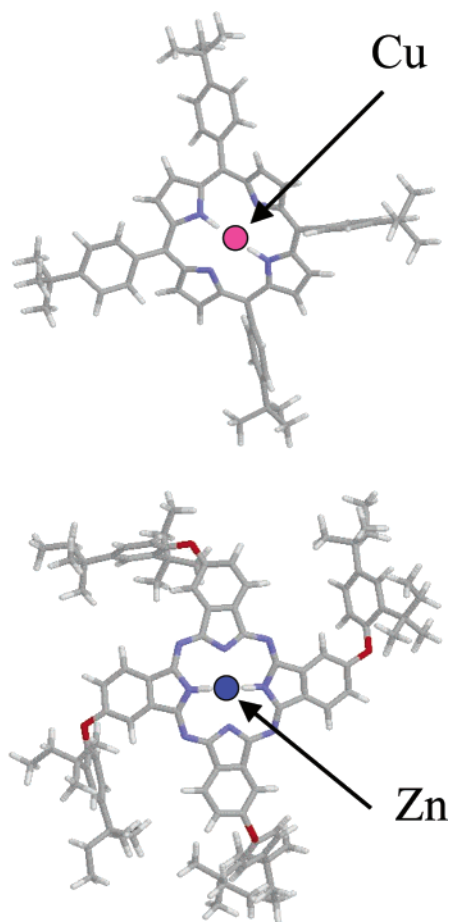


**Figure 1.** Chemical structures of  $\text{ZnPc}^{\text{tamyl}}$  and  $\text{CuPc}^{\text{tphen}}$  macromolecules.

optical fiber, and the absorption spectra (in 300–700 nm range) were collected and analyzed using a commercial spectrophotometer (AVANTES model MC 2000).

A specific experimental setup was realized to acquire simultaneously the array optical responses to gases and/or vapors in terms of the absorption curve variations in the UV–Vis spectral range. It allows also one to acquire the dynamic responses at different fixed spectral ranges where the response is a maximum. All the measurements were carried out at room temperature and at normal incidence of the light beam. The effect of the VOC vapors on the absorption properties of the active layer was measured in a dynamic pressure system implemented in our laboratory where dry air at ambient pressure was used as carrier and reference gas. The spectrum  $A_0$  (absorbance in dry air) of each thin active layer was first measured in dry air flow and used as the standard reference for the absorption spectrum  $A$  of the film in the presence of vapors. Four independent sensor cells were realized in a meander section of the principal stainless steel pipeline of the gas/vapor transfer apparatus by turning Swagelok pipe connections into suitable slots for sensors. For each slot there are two connectors for the connections of two optical fibers, one linked to the light source and the other to the spectrophotometer. In this way all the sensors can be exposed to the same gas or vapor concentration under the same experimental conditions.

In particular, for the optical analysis of the volatile organic compounds considered in this work, the corresponding liquid VOC samples (10 mL) were introduced into 20 mL vials kept at room temperature by a thermostatic tank. We considered the following VOCs: methanol, ethanol, isopropyl alcohol, *N,N*-diethylaniline, pyridine, 2-bromopyridine, hexane, acetone, and *tert*-butylamine. To evaluate the optical sensor response (in terms of absorbance spectrum variation) to the considered VOCs, a dry air flow (total flow of 20 sccm) was deviated in

the vial for collecting the saturated vapor of each VOC. The obtained concentration of the VOC saturated vapor depends on its saturated vapor pressure and the temperature at which the liquid sample is kept. Due to the different saturated vapor pressures (SVP) of the considered VOCs at room temperature, the concentration of the so produced saturated vapors is different for each VOC. To obtain an equal concentration for all the VOCs sent in the test chambers, the air flow carrying the saturated vapors was diluted to the reference flow of dry air in different suitable ratios for each VOCs. The gas mixing station consists of a mass flow controller (MKS Instruments model 647B) equipped with two mass flow meters/controller (MFCs) and a system of stainless steel pipelines and switching valves.<sup>21</sup> The experimental procedure started by flowing dry air through the sample chamber until a steady absorbance reading was obtained. Next, for each VOC the fixed concentration of vapors was transferred into the sensor test cells realized in the meander pipe as described above. The mentioned experimental setup allows the simultaneous monitoring of the UV–Vis spectrum variations in four defined spectral ranges covering the whole spectrum of the sensing layer.

The selected wavelength intervals were chosen by taking into account the spectral features observed in the mixed sensing layer for obtaining of the highest variations of the integrals, a reasonable signal-to-noise ratio, and the implementation of commercial light sources such as light-emitting diodes. So the 300–700 nm spectrum was divided into four spectral intervals,  $\Delta\lambda_1 = 300\text{--}400$  nm,  $\Delta\lambda_2 = 400\text{--}450$  nm,  $\Delta\lambda_3 = 500\text{--}550$  nm, and  $\Delta\lambda_4 = 550\text{--}700$  nm, and the related integrals of the absorbance were called, respectively,  $I_1$ ,  $I_2$ ,  $I_3$  and  $I_4$ . The first interval  $\Delta\lambda_1$  is of interest because of the presence of the  $\text{ZnPc}^{\text{tamyl}}$  B band, centered at about 350 nm, the second interval  $\Delta\lambda_2$  is related to the  $\text{CuPc}^{\text{tphen}}$  Soret band (420 nm), and the remaining intervals  $\Delta\lambda_3$  and  $\Delta\lambda_4$  monitor the variations occurring in the Q broad absorption band centered between 500 and 550 nm spectral range of the porphyrin macromolecules, whereas the 550–700 nm spectral interval is connected with the Q-band of phthalocyanine macromolecules.

### 3. Results and Discussion

**3.1. AFM Surface Topography.** In Figure 2 the surface topography of  $\text{ZnPc}^{\text{tamyl}}$  and  $\text{CuPc}^{\text{tphen}}$  films deposited by spin-coating onto quartz substrate is shown. In particular, 2D and 3D views of  $\text{ZnPc}^{\text{tamyl}}$  (Figure 2a,b) and  $\text{CuPc}^{\text{tphen}}$  (Figure 2c,d) films are reported, both for scan size  $5\ \mu\text{m} \times 5\ \mu\text{m}$ . The surface of  $\text{ZnPc}^{\text{tamyl}}$  film contains open structures, about 700 nm wide, which repeat themselves regularly on different regions of the surface. The root mean square (rms) roughness value is about 1.1 nm. Instead, the surface of the  $\text{CuPc}^{\text{tphen}}$  film is very irregular and contains many aggregates with a rms roughness value of 11.4 nm. Figure 3 shows the surface topography of the blend system ( $\text{ZnPc}^{\text{tamyl}}\text{--CuPc}^{\text{tphen}}$ ) deposited by spin-coating onto quartz substrate. In particular, Figure 3a,b report AFM 2D and 3D images of the film morphology for a scan size area of  $5\ \mu\text{m} \times 5\ \mu\text{m}$ . The surface of the film does not contain aggregates, but it shows open structures, 700 nm wide, which repeat themselves regularly on the entire surface. The rms roughness value is about 1.1 nm. So, the blend system ( $\text{ZnPc}^{\text{tamyl}}\text{--CuPc}^{\text{tphen}}$ ) morphology resembles the  $\text{ZnPc}^{\text{tamyl}}$  one. However, all these structures guarantee a high ratio surface/volume and, consequently, the presence on the surface of an interesting distribution of adsorption sites disposable for vapor–surface interaction.

(21) Spadavecchia, J.; Ciccarella, G.; Rella, R.; Capone, S.; Siciliano, P. *Sens. Actuators B*, in press.

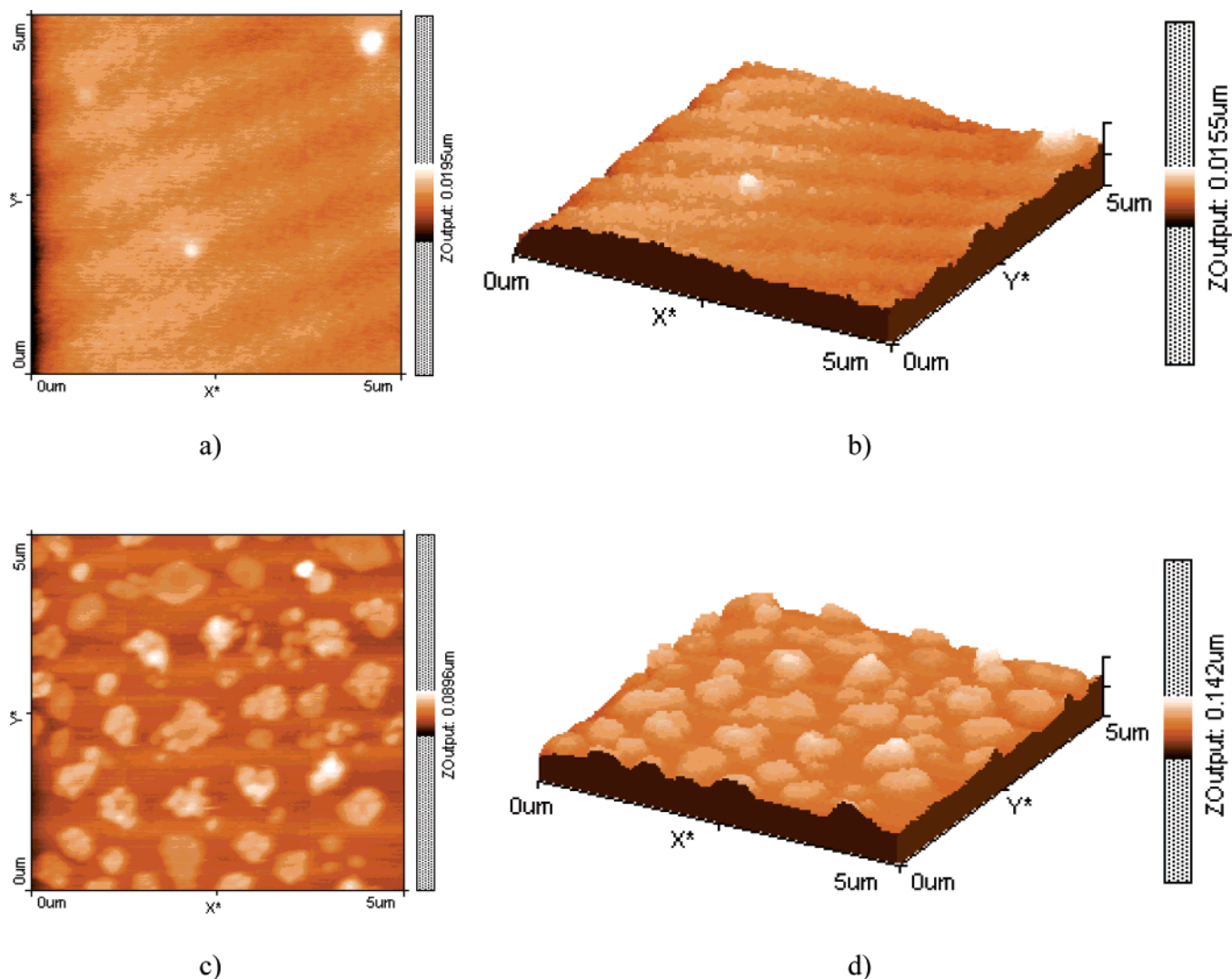


**Figure 2.** AFM images of  $\text{ZnPc}^{\text{tamyI}}$  and  $\text{CuP}^{\text{tphen}}$  spin-coated films. Plane views (a and c) and 3D views (b and d) of the films surface.

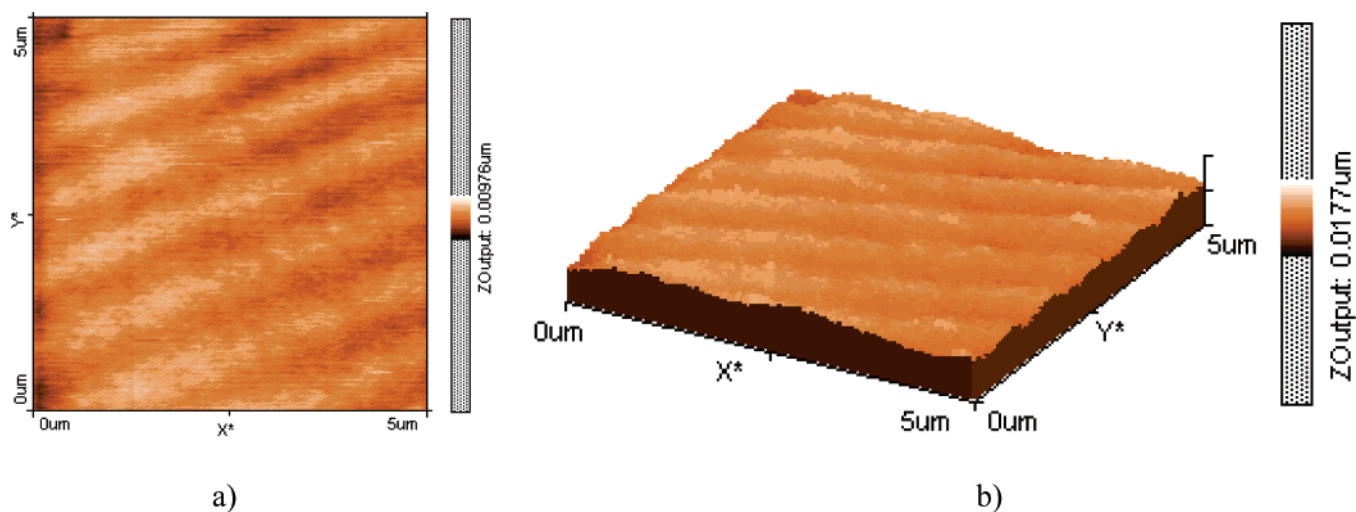


**Figure 3.** AFM images of the spin-coated film of the blend system ( $\text{ZnPc}^{\text{tamyI}}-\text{CuP}^{\text{tphen}}$ ). Plane view (a) and 3D view (b) of the film surface.

**3.2. Spectrophotometric Measurements.** Figure 4 reports typical optical absorption spectra of the  $\text{CuP}^{\text{tphen}}-\text{ZnPc}^{\text{tamyI}}$  blend in chloroform solution compared with the corresponding absorption spectrum of the spin-coated film. As one can see, the solution of the

mixed structure is characterized by an intense Soret band at 417 nm and a smaller Q band at 540 nm due to the  $\text{CuP}^{\text{tphen}}$  macromolecule, whereas the contribute of the  $\text{ZnPc}^{\text{tamyI}}$  system is characterized by a B band at 344 nm related to the energy of the  $n-\pi^*$  bands

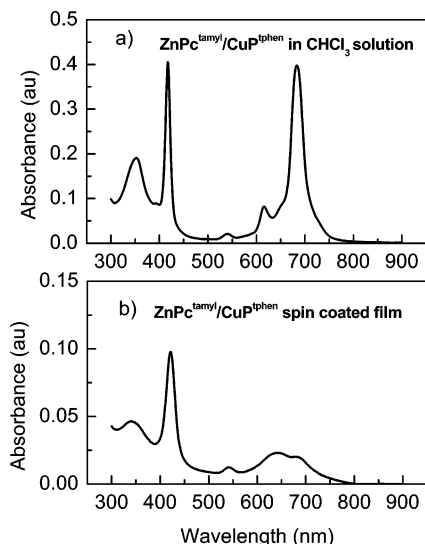


**Figure 4.** UV-Vis absorption spectra of the (a)  $\text{ZnPc}^{\text{tamyl-}}$ - $\text{CuP}^{\text{tphen}}$  blend in  $\text{CHCl}_3$  solution and (b)  $\text{ZnPc}^{\text{tamyl-}}$ - $\text{CuP}^{\text{tphen}}$  spin-coated thin film.

associated with the nitrogen lone pair orbital of the phthalocyanine ring and two main bands,  $Q_I$  ( $\lambda_{\text{max}} = 683$  nm) and  $Q_{II}$  ( $\lambda_{\text{max}} = 616$  nm). The spin-coated film spectrum puts in evidence the variation of the  $\text{ZnPc}^{\text{tamyl}}$  Q bands: a broad band centered at 642 nm is typically due to the phthalocyanine dimers or higher aggregates, whereas the 680 nm shoulder is related to the monomer and corresponds to the  $Q_I$  band found in the solution spectrum. The Soret band of the porphyrin results also broadened and slightly red-shifted to 421 nm. The decrease in the area under the absorption peak of the thin film in the 600–700 nm spectral range and corresponding to the phthalocyanine Q-band is due to the different extinction coefficient characteristic of the  $\text{CuP}^{\text{tphen}}$  with respect to the  $\text{ZnPc}^{\text{tamyl}}$  macromolecules.

**3.3. Optical Sensing Characteristics.** The construction of a mixed system of phthalocyanines–porphyrins for sensory application represented for us an appealing object of investigation, because of the possibility to obtain some unique variations of the hybrid material itself by variations of the  $\text{ZnPc}^{\text{tamyl-}}$ - $\text{CuP}^{\text{tphen}}$  molar ratio with respect to covalently linked heterodimers or a double-decker heterocomplex of defined stoichiometry. The interactions between the two macrocycles may induce some variation of the coordination ability in the central metal ions toward the tested analytes, and different molecular packing in the solid state can be also supposed. As a consequence, a different response toward the investigated VOCs, with respect to those found with  $\text{ZnPc}^{\text{tamyl}}$  and  $\text{CuP}^{\text{tphen}}$  homolayers, is observed. Figures 5 and 6 show the dynamic responses corresponding to the variation in the absorbance intensity on four independent channels. In particular,  $I_1$ ,  $I_2$ ,  $I_3$ , and  $I_4$  reported in the figures are values corresponding to the calculus of the area integral under the selected peaks for well-defined wavelength range carried out in dry air and in the presence of a mixture of dry air and *tert*-butylamine vapors in the controlled concentrations inlet in each test chamber. Similar measurements have been collected for all the analyzed vapors. Different dynamic curves have been obtained; each of them shows different responses. The evidence of these variations is confirmed by the values of the

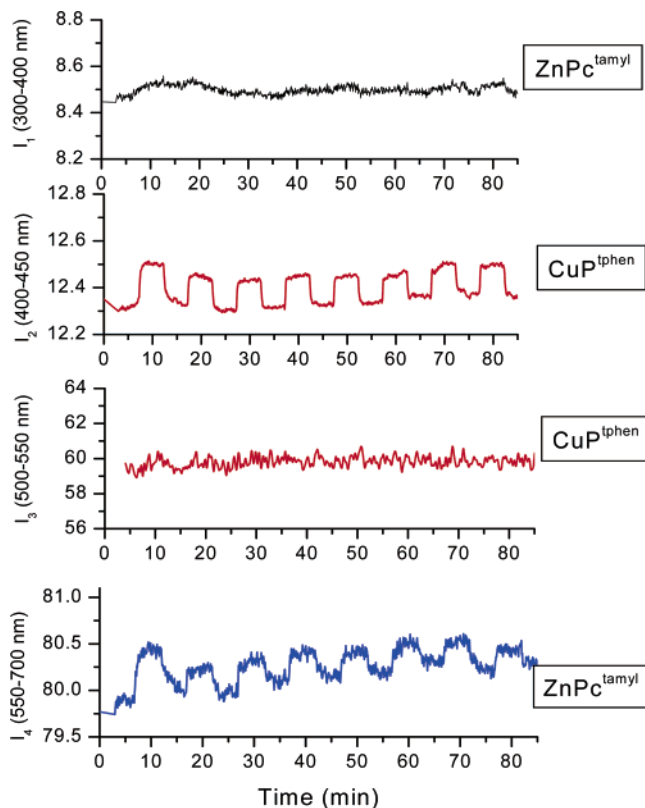


**Figure 5.** Typical dynamic responses referred to the four channels ( $I_1$ ,  $I_2$ ,  $I_3$ , and  $I_4$ ) for the S1 system in the presence of *tert*-butylamine vapors.

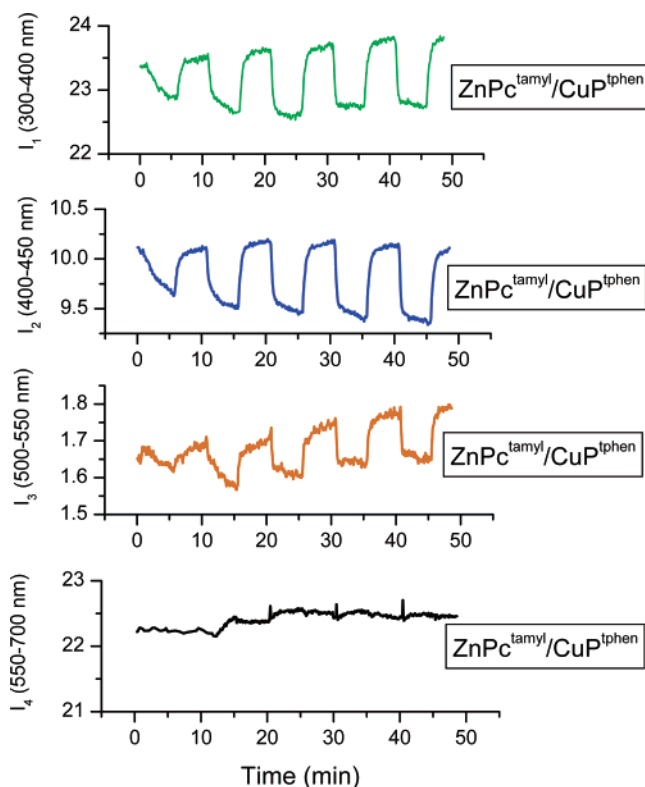


**Figure 6.** Typical dynamic responses referred to the four channels ( $I_1$ ,  $I_2$ ,  $I_3$ , and  $I_4$ ) for the S2 system in the presence of *tert*-butylamine vapors.

responses  $R_n$  calculated as the difference  $R_n = (I_n - I_0)$ , where  $I_n$  is the integral measured in the presence of the VOC vapors and  $I_0$  is the integral measured in dry air

**Table 1. Responses  $R_n = I_n - I_0$  Calculated from Experimental Data Obtained with the CuP<sup>tphen</sup> and ZnPc<sup>tamy1</sup> Sensing Layers Interacting with the Different VOCs (data set S1)<sup>a</sup>**

S1	MeOH	EtOH	IPA	acetone	TBA	NNDEA	Py	2-BrPy	hex
$R_1$									
$R_2$			0.2						-0.1
$R_3$	0.2	0.4	0.5	0.2	0.1	-0.2	0.2	0.2	
$R_4$	0.4	0.8	1.5	0.3	0.3	-0.4	0.3	0.4	-0.2

<sup>a</sup> MeOH = methanol, EtOH = ethanol, IPA = isopropanol, TBA = *tert*-butylamine, NNDEA = *N,N*-diethylaniline, Py = pyridine, 2-BrPy = 2-bromopyridine, hex = hexane.

**Table 2. Responses  $R_n = I_n - I_0$  Calculated from Experimental Data Obtained with the CuP<sup>tphen</sup>-ZnPc<sup>tamy1</sup> Blend Sensing Element Interacting with the Different VOCs (data set S2)**

S2	MeOH	EtOH	IPA	acetone	TBA	NNDEA	Py	2-BrPy	hex
$R_1$			0.3	-0.2	-1.1				-0.1
$R_2$		0.1	0.3		-0.7				-0.1
$R_3$									
$R_4$	0.5	0.5	1.0	-0.2		0.3	0.1	-0.3	0.3

<sup>a</sup> MeOH = methanol, EtOH = ethanol, IPA = isopropanol, TBA = *tert*-butylamine, NNDEA = *N,N*-diethylaniline, Py = pyridine, 2-BrPy = 2-bromopyridine, hex = hexane.

flux. Table 1 represents the responses toward the different analytes of the single porphyrin and the phthalocyanine active layers (data set S1). In particular,  $R_2$  and  $R_3$  are the responses of the porphyrin-based sensing element;  $R_1$  and  $R_4$  are the responses related to the phthalocyanine-based sensing element. The first data set can be considered as the first sensing system and it will be called S1. In Table 2 the responses of a new sensing system (data set S2) based on the porphyrin-doped Pc layer are reported. The histograms shown in Figure 7a,b represent the responses  $R_n$  vs the different analytes. As one can see, both positive and negative values of  $R_n$  are possible, depending on the variation of the absorption bands of the sensing element<sup>17</sup> when exposed to the analyte vapors. The choice to calculate the responses in terms of the difference in the dynamic integrals is due to the consideration that each absorption peak is proportional to the number of active macromolecules in the sensing process. The sensing mechanism involves a portion of these complexes by an increase or decrease of the peak area; consequently, we stress that the difference in the integral gives a better evaluation of the sensing phenomenon. Moreover, the gas–solid interaction of the VOCs under analysis with the spin-coated films produced changes in the optical absorption spectra of the films and, in particular, a variation in the absorption intensity of the typical Q and Soret bands of these macromolecular systems. Very interesting results have been obtained concerning the response and recovery times of our systems, defined as the 90% variation in the integral area signal in the presence of vapors in the test chamber and 10% from the equilibrium value in the presence of dry-air, respectively. In particular, they have been estimated to be about 3 min. Moreover, all the optical tests performed in controlled atmosphere have been carried out at room temperature; consequently, the obtained response time and recovery time depend on the temperature of the measurements.

The interaction mechanism responsible for the optical responses of the thin films of phthalocyanines or por-

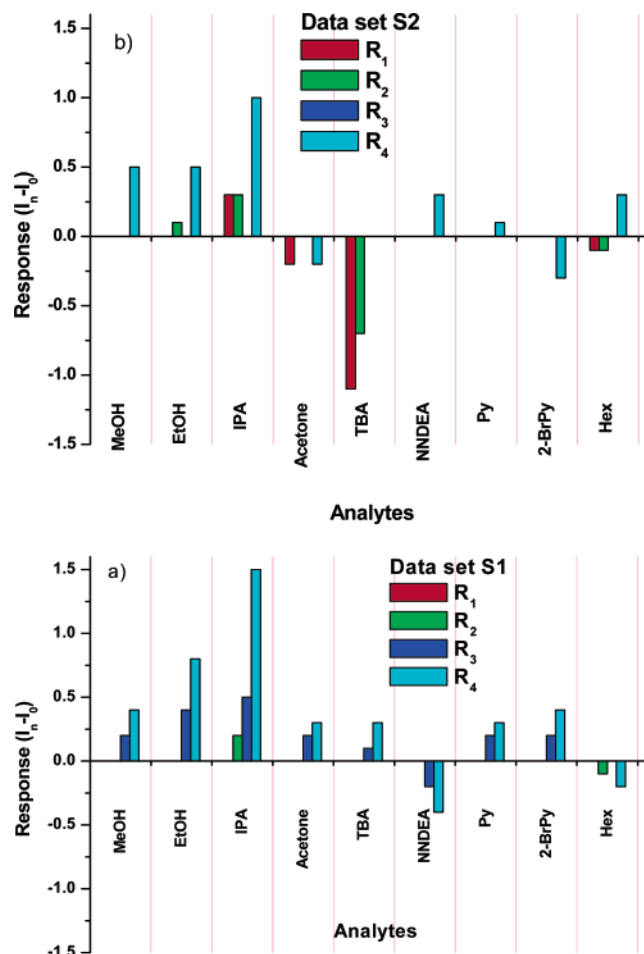


**Figure 7.** (a) Histogram of the responses  $R_n$  obtained in the presence of different analytes using ZnPc<sup>tamy1</sup> and CuP<sup>tphen</sup> thin films as sensing layers. (b) Histogram of the responses  $R_n$  obtained in the presence of different analytes using porphyrin-doped ZnPc<sup>tamy1</sup> thin film as sensing layer.

phyrins versus gases has not been so extensively studied. Securely, the exposure of these organic materials in the thin film form to VOCs leads to variations in the electronic density in the molecular units of the film such as to justify a variation in the optical absorption peaks. Consequently, an increase or decrease in the absorption peaks could be due to a variation in the density of free electrons available for optical transition corresponding to the Q and Soret bands. In particular, a decrease in the intensity of a specific absorption band is consistent with the formation of a charge-transfer complex between the phthalocyanine and the VOCs.

**3.3.1. Sensing toward Alcohols and Acetone.** The S1 system reacts to the different alcohols' exposure with a similar behavior (Figure 7a); only 2-propanol seems to be discriminated by the porphyrin  $R_2$ , and no significant variation in the responses pattern was found for methanol and ethanol. The porphyrin-doped sensing element (data set S2) (see Figure 7b) shows a different behavior with respect to the data set S1: the 2-propanol exposure causes the rise of both porphyrin  $R_2$  and phthalocyanine  $R_4$  and  $R_1$  responses with respect to the data set S1. On the contrary, the  $R_3$  signal decreases in the ethanol recognition (data set S2), whereas a slight but however detectable  $R_2$  is observed. Moreover, methanol is detected only by phthalocyanine  $R_4$ . The interaction with acetone showed a different pattern with nega-

tive values of  $R_1$  and  $R_4$  of the data set S2 with respect to the data set S1. It is interesting to note, as in the case of the S1 data set, only  $R_3$  and  $R_4$  bands react with acetone vapors. The blend system switches off these responses and switches on  $R_1$  and  $R_2$ . Independent responses are then observed demonstrating that a suitable material manufacture with specific sensing feature can be realized.

**3.3.2. Sensing toward Amines.** A strong selectivity can be supposed by comparing the responses related with *tert*-butylamine and *N,N*-diethylaniline. The exposition of the S1 system to the vapors of these analytes causes the variation of the  $I_3$  and  $I_4$  integrals. These variations were found to be positive for the *tert*-butylamine ( $R_3$  and  $R_4$ ) and negative for the *N,N*-diethylaniline vapors ( $R_3$  and  $R_4$ ) (Figure 7a); in both cases, no significant variations were observed for the  $I_1$  and  $I_2$  integrals. The data set S2 offers a completely different situation: the exposure to *tert*-butylamine vapors causes highly negative  $R_1$  and  $R_2$  values. On the contrary, a positive  $R_4$  response was recorded with *N,N*-diethylaniline.

**3.3.3. Sensing toward Pyridine Derivatives.** Despite of the well-known ligand ability of the pyridine derivatives, the two sensing layers do not show a specific behavior. The S1 system presents similar low  $R_3$  and  $R_4$  responses for pyridine and 2-bromopyridine, whereas no  $R_3$  responses appear in the S2 data set. Finally, an inversion of the sign is observed in the case of the 2-bromopyridine.

**3.4. Data Analysis by PCA.** Once the absorbance spectra of all sensing layers tested in the presence of different VOCs were collected and the responses calculated, the data thus obtained were elaborated by a simple statistical-chemometric technique, i.e., PCA.<sup>22,23</sup>

It is worth remembering how PCA works. PCA is a powerful unsupervised linear data analysis technique widely used in gas-sensing area to extract the main relationships in the data matrix containing the sensor responses and to obtain qualitative results for pattern recognition. It projects the data in a new vectorial space of lower dimensionality, where the new axes (i.e. the principal components, PCs) are linear combinations of the original axes (sensors) and orthogonal to each other. The principal components are computed iteratively, in such a way that the first PC is the one that carries the most "information" (or, in statistical terms, the most explained data variance). Then, the second PC will be orthogonal to the first one and will carry the maximum share of the residual information (i.e. the variance not taken into account by the previous PC), and so on. Thus, only the first PCs (usually the first two or three PCs) can be preserved because they are more relevant, while the last PCs are assumed only to represent the contribution of the noise to the data. PCA operates a synthesis of the data, by removing redundant information and reducing the data space dimension. In a pictorial way, we can say that the principal components give the directions in which the data cloud is stretched most. By projecting the response data on the PCs vectorial space

(feature space), one can easily detect and analyze groupings, similarities, or differences between the samples. Two samples can be considered similar if they have close values for most variables, which means correspondingly close coordinates in the feature space. The data projection on the PCs space is, hence, useful for subsequent pattern recognition analysis, because it is easy to visualize clusters related to different chemical patterns in the feature space.

In the frame of this work, we applied PCA to our data with the aim to evaluate the discrimination power of the hybrid optosensor array based on  $\text{ZnPc}^{\text{tamyl}}$ ,  $\text{CuPt}^{\text{phen}}$ , and their blend among all nine of the considered VOCs. As feature extracted from the experimental data, we chose the optical response defined as

$$R_n = \Delta I = I_{n_i} - I_0$$

where  $I_{n_i}$  ( $i = 1, \dots, 9$  VOCs) is the integral area of the absorbance spectra in a fixed spectral range in the presence of the vapor of the  $i$ -VOCs ( $\sim 43.000$  ppm in air) and  $I_0$  is that in the presence of dry air.

We arranged the response matrix for data analysis by considering some characteristics of the optical responses of our system. In particular, we observed that in spectral range  $\Delta\lambda_1$  the  $\text{ZnPc}^{\text{tamyl}}$  layer has no appreciable spectra variations in the presence of all the considered VOC vapors, while the blend system shows good responses. On the contrary, in the spectral range  $\Delta\lambda_3$  the blend system has no appreciable spectra variations in the presence of all the considered VOC vapors, while the  $\text{CuPt}^{\text{phen}}$  layer shows good responses. In the spectral range  $\Delta\lambda_2$  both the  $\text{CuPt}^{\text{phen}}$  and the  $\text{ZnPc}^{\text{tamyl}}-\text{CuPt}^{\text{phen}}$  blend layers gave good responses to the considered VOC vapors; analogously, in the spectral range  $\Delta\lambda_4$  both the  $\text{ZnPc}^{\text{tamyl}}$  and  $\text{ZnPc}^{\text{tamyl}}-\text{CuPt}^{\text{phen}}$  blend layers gave appreciable responses. Hence, as variables for the PCA we chose (a) for  $\Delta\lambda_1$  the optical responses of only the  $\text{ZnPc}^{\text{tamyl}}-\text{CuPt}^{\text{phen}}$  blend layer, (b) for  $\Delta\lambda_2$  the optical responses of both the  $\text{CuPt}^{\text{phen}}$  and  $\text{ZnPc}^{\text{tamyl}}-\text{CuPt}^{\text{phen}}$  blend, (c) for  $\Delta\lambda_3$  the optical responses of the only  $\text{CuPt}^{\text{phen}}$ , and (d) for  $\Delta\lambda_4$  the optical responses of both  $\text{ZnPc}^{\text{tamyl}}$  and  $\text{ZnPc}^{\text{tamyl}}-\text{CuPt}^{\text{phen}}$  blend. In this way, six variables containing the responses of our selected system toward all the considered VOC vapors have been used for PCA.

To collect enough data to perform a PCA, five cycles of VOC-sensing tests, consisting of an exposure to each VOC vapor and a subsequent recovery in dry air, have been carried out. This procedure gave us also the possibility to check the reproducibility of the responses. Hence, five response values for each of the nine VOC vapors and each of the six selected variables have been collected; a data matrix of 40 samples and six variables have been thus used as input to the PCA algorithm.

The Figure 8 shows the score plots of PCA analysis based on the responses of our hybrid optosensor array to the considered analytes in the selected spectral ranges. In particular, Figure 8a shows the three-dimensional data representation in the vectorial space of the first three principal components, while in parts b and c of Figure 8 the projections on the plane PC1-PC3 and PC1-PC2 are reported, respectively. First, we can note that over 85% and 95% of the total variance within the data is contained in the first two and the

(22) Gardner, J. W. *Sens. Actuators, B* **1991**, *B4*, 109–115.

(23) Gardner, J. W.; Bartlett, P. N. Pattern recognition in gas sensing. In *Techniques and Mechanisms in Gas Sensing*; Moseley, P. T., Norris, J. O. W., Williams, D. E., Eds.; Adam Hilger: Bristol, 1991; pp 347–379.

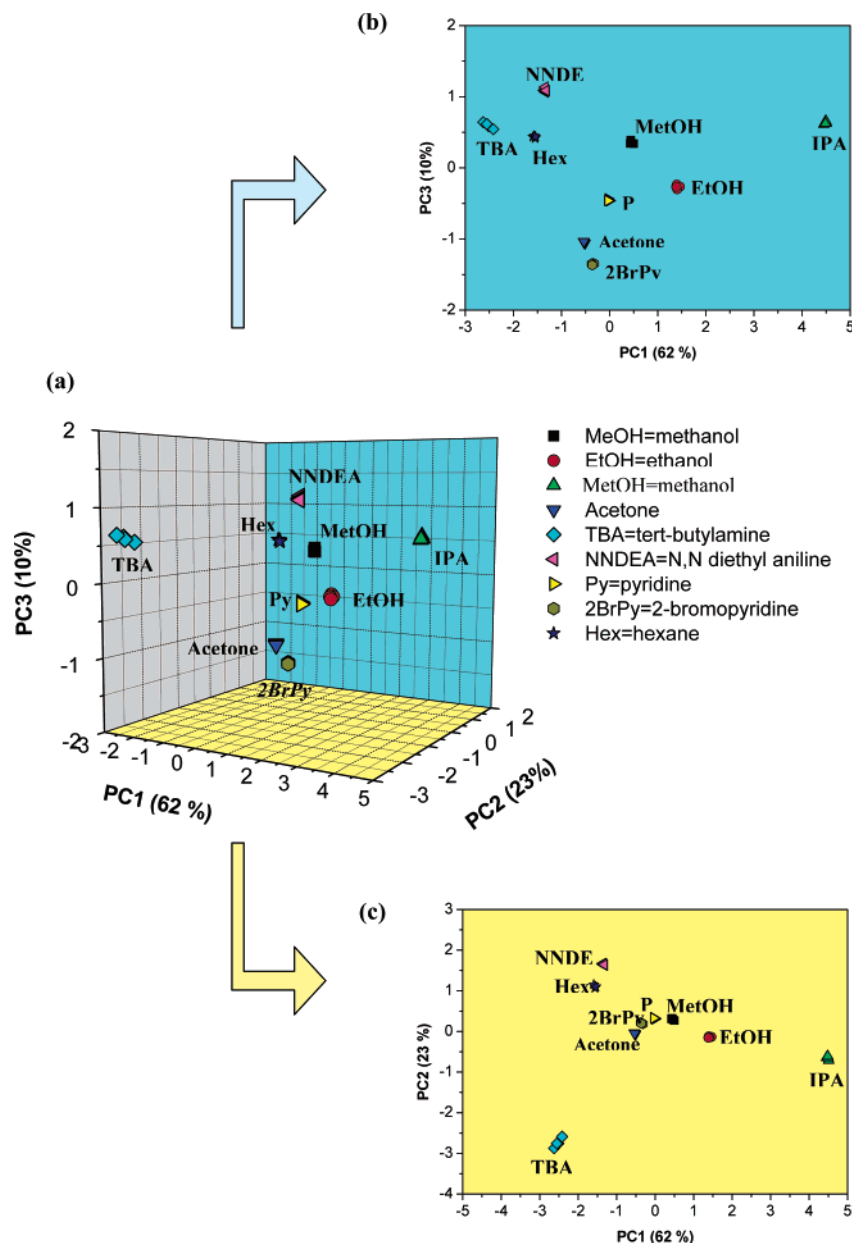


**Figure 8.** (a) PCA 3D score plot related to the responses of the array optical sensors corresponding to the blend and homolayers active systems. Projections on the plane (b) PC3–PC1 and (c) PC2–PC1.

first three principal components, respectively. Moreover, a good discrimination among the different VOC vapors was obtained. In fact, a satisfactory separation among the different data clusters in the PC-vectorial space is clearly evident. The experimental points corresponding to the same analyte are also well closed so that the data spread is minimal.

### Conclusions

In this work we reported the optochemical sensing properties of a porphyrin-doped phthalocyanine spin-coated layer (S2) compared with those related to two single-species thin films (S1). Optical and morphological characterization of the realized thin films has been performed and reproducibility of the layers confirmed. The UV–Vis spectra of each system were divided into four intervals in order to monitor the spectral variations in optical absorbance in the presence of some volatile organic compounds by means of the related integrals of the absorbance. This particular arrangement has been

considered as an array of independent sensors located on a single sensing material. The results of our investigation can be considered really encouraging if we consider that the goal of our work was to optimize a hybrid optosensor array. Typical optical absorption peaks corresponding to the Q and Soret bands of phthalocyanines and porphyrins generate an array of four independent sensors. Principal component analysis has been performed in order to test the capacity of the array to discriminate between different classes of VOCs of interest in food quality control.

Further studies concerning the optimization of the thin layers in term of thickness and composition will be reported soon together with the analysis of a mixture of volatile organic vapors.

**Acknowledgment.** Many thanks are due to Mr. F. Casino and Mrs. C. Martucci for skillful technical assistance with the experimental setup.

CM034871U